


Quantifying Subclinical and Longitudinal Microvascular Changes Following Episcleral Plaque Brachytherapy Using Spectral Domain–Optical Coherence Tomography Angiography

Journal of VitreoRetinal Diseases
2020, Vol. 4(6) 499-508
© The Author(s) 2020
Article reuse guidelines:
sagepub.com/journals-permissions
DOI: 10.1177/2474126420936199
jvrd.sagepub.com



Kyle M. Green, MD¹, Brian C. Toy, MD¹, Bright S. Ashimatey, OD, PhD¹,
Debarshi Mustafi, MD, PhD¹, Richard L. Jennelle, MD², Melvin A. Astrahan, PhD²,
Zhongdi Chu, PhD³, Ruikang K. Wang, PhD^{3,4}, Jonathan Kim, MD^{1,5},
Jesse L. Berry, MD^{1,5}, and Amir H. Kashani, MD, PhD^{1,6} 

Abstract

Purpose: This work assesses longitudinal microvascular changes in eyes treated with iodine-125 episcleral plaque brachytherapy (EPB). **Methods:** High-resolution optical coherence tomography angiograms (OCTAs) of the central 3 × 3-mm macula were obtained from iodine-125 EPB-treated and untreated fellow eyes of 61 patients. Previously validated semiautomated algorithms quantified capillary density (vessel skeleton density [VSD]) and caliber (vessel diameter index). Nonperfusion was also quantified as flow impairment region (FIR). Examinations from treated and fellow eyes obtained before treatment and at 6-month, 1-year, and 2-year intervals were compared using generalized estimating equation linear models. Dosimetry maps evaluated spatial correlation between radiation dose and microvascular metrics. **Results:** At 6 months, treated eyes had significantly lower VSD (0.145 ± 0.003 vs 0.155 ± 0.002 ; $P = .009$) and higher FIR (2.01 ± 0.199 vs 1.46 ± 0.104 ; $P = .01$) compared with fellow eyes. There was a significant decrease in VSD and a corresponding increase in FIR even for treated eyes without clinically identifiable retinopathy at 6 months. Vessel diameter index was significantly higher in treated eyes than in fellow eyes at 2 years (2.92 ± 0.025 vs 2.84 ± 0.018 ; $P < .001$). We categorized our cohort into low-dose (< 15 Gy) and high-dose (> 45 Gy) radiation to the fovea and noted significant differences in VSD and FIR between groups. **Conclusions:** OCTA can quantify and monitor EPB-induced retinopathy and can detect vascular abnormalities even without clinically observable retinopathy. OCTA may be useful in investigating treatment interventions aiming to delay EPB-induced radiation retinopathy.

Keywords

optical coherence tomography angiography, episcleral plaque brachytherapy, choroidal melanoma, capillary, biomarker, radiation retinopathy

Introduction

The development of radiation retinopathy (RR) following treatment of choroidal melanoma with episcleral plaque brachytherapy (EPB) can have deleterious effects on retinal microvasculature that lead to permanent visual decline. The Collaborative Ocular Melanoma Study validated EPB as the standard of care for globe-conserving treatment of medium-sized choroidal melanomas.¹ Despite the selection of iodine-125 and gold shielding to minimize adverse radiation effects, visual morbidity remains high, with only 43% of patients maintaining visual acuity (VA) of 20/200 or better 3 years after treatment with standard Collaborative Ocular Melanoma Study plaques.²

Some reports indicate that adverse radiation effects can be partially mitigated through the use of 3-dimensional conformal

¹ Department of Ophthalmology, Keck School of Medicine, USC Roski Eye Institute, University of Southern California, Los Angeles, CA, USA

² Department of Radiation Oncology, University of Southern California Norris Comprehensive Cancer Center, Los Angeles, CA, USA

³ Department of Bioengineering, University of Washington, Seattle, Washington, USA

⁴ Department of Ophthalmology, University of Washington, Seattle, Washington, USA

⁵ The Vision Center, Children's Hospital Los Angeles, Keck School of Medicine, Los Angeles, CA, USA

⁶ USC Ginsburg Institute for Biomedical Therapeutics, University of Southern California, Los Angeles, CA, USA

Corresponding Author:

Amir H. Kashani, MD, PhD, USC Ginsburg Institute for Biomedical Therapeutics, University of Southern California, 1450 San Pablo St, 6th Fl, Los Angeles, CA 90033, USA.

Email: ahkashan@usc.edu

treatment-planning software and customized collimated plaques to decrease the radiation dose to critical visual structures (eg, the fovea).^{3,4} The onset of RR varies greatly, ranging from as early as 1 month to 15 years, but it most commonly occurs between 6 months and 3 years after treatment.⁵ The location of the tumor, and thus the dose to the fovea, is critical but not the sole risk factor. RR is primarily a vascular disease and shares many clinical features with diabetic retinopathy (DR) including damage to capillaries, which leads to variable degrees of hyperpermeability, retinal ischemia, and neovascularization.⁶

Although clinical features of RR, including dot-blot hemorrhages, microaneurysms, and macular edema (ME), can be seen on examination, as with DR, there is underlying damage present before these clinical features manifest. Fluorescein angiography can reveal early areas of nonperfusion and vascular leakage.⁷⁻⁹ Optical coherence tomography angiography (OCTA) has been used to noninvasively demonstrate morphologic features of microvasculature with excellent spatial resolution.¹⁰⁻¹³ By generating detailed depth-resolved images, OCTA can potentially be used to detect and monitor capillary-level aberrations in blood flow at multiple time points early in the course of RR. To date, there have been a few studies that used OCTA to assess microvascular changes in RR. Two recent studies used binarized OCTA to demonstrate a decrease in parafoveal^{14,15} and peripapillary capillary^{16,17} density in irradiated eyes compared with fellow eyes. To our knowledge, no studies have performed longitudinal analysis to identify early microvascular changes (prior to 1 year) in treated eyes, nor have any used OCTA to explore a possible spatial correlation between these changes and radiation dose.

In the present study, we used longitudinal analysis of OCTA to further determine what quantifiable morphologic differences exist in the microvasculature between treated and fellow eyes over time, as well as elucidated whether these changes can be detected as early as 6 months postoperatively. More specifically, we used previously described OCTA metrics^{11,18} vessel skeleton density (VSD) and vessel diameter index (VDI) to quantitatively assess changes in retinal vascular networks. We have previously used these metrics to quantify vascular density and diameter in DR and uveitis.^{11,13} We also report flow impairment region (FIR), which is further detailed in the Methods section, to quantify areas of subclinical nonperfusion larger than a set threshold.

Methods

This was a retrospective, consecutive series of 61 adult patients treated with iodine-125 EPB for medium-sized choroidal melanoma by 1 of 2 ocular oncologists (J.L.B. and J.K.) at the University of Southern California Roski Eye Institute. Any participant with a history of intraocular melanoma and plaque brachytherapy was eligible for inclusion. Treatment planning and surgery were performed as previously described with a stereotactic plaque brachytherapy radiation treatment-planning platform (Plaque Simulator; Eye Physics, LLC); a dose of 85 Gy at a rate of 0.5 Gy/h was prescribed to the apex of the lesion

or to 5 mm in height, whichever was greater, with a 2-mm margin at the base.¹⁹ Individuals with media opacity impairing visualization of the macula, preexisting retinal vascular disease (eg, DR, retinal vein occlusion, or choroidal neovascularization), or preexisting subretinal fluid or ME prior to plaque placement were excluded from the study. Individuals with direct tumor involvement in the 3 × 3-mm perifoveal region were also excluded from the cohort analysis.

Patient demographics, including age and sex, were abstracted from the medical record. Clinical data collected included VA, radiation dose to fovea, follow-up time, and presence of clinically evident RR as determined by the Finger and Kurli criteria.⁸ VA was reported as logarithm of the minimum angle of resolution.

OCTA Imaging and Image Analysis

At the clinician's discretion, OCTA was performed on irradiated eyes and the fellow nonirradiated eyes of patients prior to treatment and at their postoperative follow-up visits. Imaging was performed with a commercially available, Food and Drug Administration–approved, spectral-domain OCTA platform (AngioPlex 5000, Zeiss Meditec). High-resolution 3 × 3-mm OCTAs centered on the fovea with a signal strength greater than 7 (of a 10-point scale) were included for analysis. All OCTAs were generated from full-thickness retina to avoid segmentation errors. Images with significant motion artifacts that obscured the vascular architecture were excluded from analysis. For any eye with multiple images on a single date, the highest-quality image was chosen.

A previously described semiautomated algorithm was used for quantitative analysis of VSD, VDI, and FIR.^{11,18} Briefly, VSD is defined as a unitless proportion of the total length (in pixels) of all skeletonized vessels divided by the total number of pixels in the image window; it indicates reflects capillary density. VDI is defined as a unitless proportion of the total vessel area divided by the total skeletonized vessel area; it indicates average vessel diameter. Last, FIR is defined as the sum of avascular areas in an image larger than a predefined threshold area, which in this study was set at 0.002 mm² to reflect the maximum threshold for physiologic intercapillary distance. This value was based on an estimate from histologic analysis in which the avascular periarteriolar region was approximately 50 μm.²⁰ A 0.002-mm² threshold closely approximates the area of a circle with this diameter.

Data Analyses

The effect of radiation therapy on the OCTA metrics (VSD, FIR, and VDI) was assessed longitudinally. Acquired data included pretreatment examinations obtained prior to EPB surgery, as well as examinations obtained up to 30 months postoperatively. Given the retrospective nature of our study, the postoperative follow-up dates over this period were not standardized. Therefore, for our analysis we opted to bin posttreatment examinations into intervals appropriate for the available data as follows: 6

Table 1. Patient Demographics and Clinical Data.

Total No. participants	61
Age, y	
Mean \pm SD	62.8 \pm 13.9
Median (IQR)	65.6 (56.8-73.1)
Female sex (%)	34 (55.7)
Follow-up time, y	
Mean \pm SD	0.8 \pm 0.5
Median (IQR)	0.8 (0.4-1.3)
No. with diabetes without retinopathy (%)	6 (9.8)
No. with hypertension (%)	19 (31.1)
No. that received anti-VEGF after treatment (%)	6 (9.8)
Time from plaque to first OCTA, y	
Mean \pm SD	1.3 \pm 0.8
Median (IQR)	1.3 (0.5-1.9)
Tumor and treatment characteristics	
Dose at tumor apex, mean \pm SD, median (IQR), Gy	99.7 \pm 25.3, 86.8 (85-111)
Dose at fovea, mean \pm SD, median (IQR) Gy ^a	60.3 \pm 73.0, 31.9 (17-75)
No. participants with tumors within 2 disc diameters of fovea (%)	19 (31.1)
No. participants with tumors that overlap vascular arcades (%)	19 (31.1)
Preoperative tumor apex thickness, mm	
Mean \pm SD	4.3 \pm 2.4
Median (IQR)	3.8 (2.9-4.8)

Abbreviations: anti-VEGF, antivascular endothelial growth factor; IQR, interquartile range; OCTA, optical coherence tomography angiography.

^aThe median radiation dose to the fovea (32 Gy) is less than published thresholds for clinically evident radiation damage (35 Gy).

months (range, 3-9 months), 1 year (range, 9-18 months), and 2 years (range, 18-30 months). Summary OCTA metrics were compared between irradiated and fellow eyes at the different time intervals using generalized estimating equation (GEE) linear regression models. In the GEE models, the OCTA metrics were each used as predictor variables of the treatment status of the eyes—irradiated eye vs fellow eye. Summary OCTA metrics for treated eyes were also compared between baseline and the various follow-up time points. Statistical significance was defined when the *P* value of the univariate model was less than .05. GEE models allowed for the analysis of longitudinal repeated measures and correlated fellow-eye data.²¹

In addition to the previously described analysis, we sought to explore the potential effects of hypertension and diabetes without retinopathy on our results. Because patients with diabetes composed a small portion of our cohort, we performed the same binned analysis as described earlier after excluding all people with diabetes from our cohort for purposes of comparison. Because patients with hypertension composed a larger portion of the cohort, we used a GEE regression model with age, hypertension, and VSD as the independent variables and development of clinically evident RR as the dependent variable. This model also accounted for time from plaque placement.

Table 2. Clinical and Optical Coherence Tomography Angiography Measures by Eye.

Mean \pm SEM	EPB treated	Fellow eye	<i>P</i> ^a
No. of OCTAs analyzed			
Pretreatment	14	19	
6 mo	13	19	
12 mo	15	15	
24 mo	13	19	
BCVA, logMAR			
Pretreatment	0.26 \pm 0.05	0.08 \pm 0.02	.001
6 mo	0.25 \pm 0.08	0.06 \pm 0.03	.02
12 mo	0.30 \pm 0.08	0.05 \pm 0.02	.003
24 mo	0.41 \pm 0.10	0.11 \pm 0.07	.005
Vessel skeleton density			
Pretreatment	0.152 \pm 0.003	0.155 \pm 0.002	.26
6 mo	0.145 \pm 0.003	0.155 \pm 0.002	.009
12 mo	0.143 \pm 0.005	0.157 \pm 0.003	.02
24 mo	0.143 \pm 0.005	0.155 \pm 0.002	.04
Vessel diameter index			
Pretreatment	2.85 \pm 0.020	2.86 \pm 0.012	.97
6 mo	2.86 \pm 0.023	2.85 \pm 0.016	.65
12 mo	2.91 \pm 0.043	2.83 \pm 0.013	.08
24 mo	2.92 \pm 0.025	2.84 \pm 0.018	.001
Flow impairment region			
Pretreatment	1.65 \pm 0.175	1.49 \pm 0.120	.41
6 mo	2.01 \pm 0.199	1.46 \pm 0.104	.01
12 mo	2.19 \pm 0.243	1.48 \pm 0.168	.03
24 mo	2.08 \pm 0.267	1.49 \pm 0.087	.03

Abbreviations: BCVA, best-corrected visual acuity; EPB, episcleral plaque brachytherapy; logMAR, logarithm of the minimum angle of resolution; IQR, interquartile range; OCTA, optical coherence tomography angiography.

^aBold font indicates significance defined at an alpha level of .05.

Radiation Dose Response Analysis

Radiation dose-related changes of the OCTA metrics were also investigated in 2 ways. The OCTA metrics between high-dose eyes (foveal radiation >45 Gy) were compared with low-dose eyes (foveal radiation <15 Gy). These thresholds were chosen based on published dose tolerance limits of the retina.²²

A second exploratory approach was adopted to assess whether there was spatial correlation between radiation dose and microvascular density within the 3 \times 3-mm foveal region of an individual eye. Because the main goal of EPB is to treat the tumor with minimal radiation exposure to the foveal and optic nerve regions, high-dose gradients to the foveal 3 \times 3-mm area were possible only for lesions located very close to or including the fovea. Therefore, for this analysis, the participant criteria were modified to include individuals with the greatest radiation dose gradient to the 3 \times 3-mm foveal region irrespective of lesion location.

To evaluate this within-eye correlation, the last acquired OCTAs (over the defined study period) of the irradiated eyes were investigated, and 5 eyes that displayed the largest spatial gradients in microvascular density were selected for further evaluation. EPB dosimetry maps of these eyes were then generated using Eye Physics Plaque Simulator software (Eye Physics, LLC), developed previously at the University of Southern

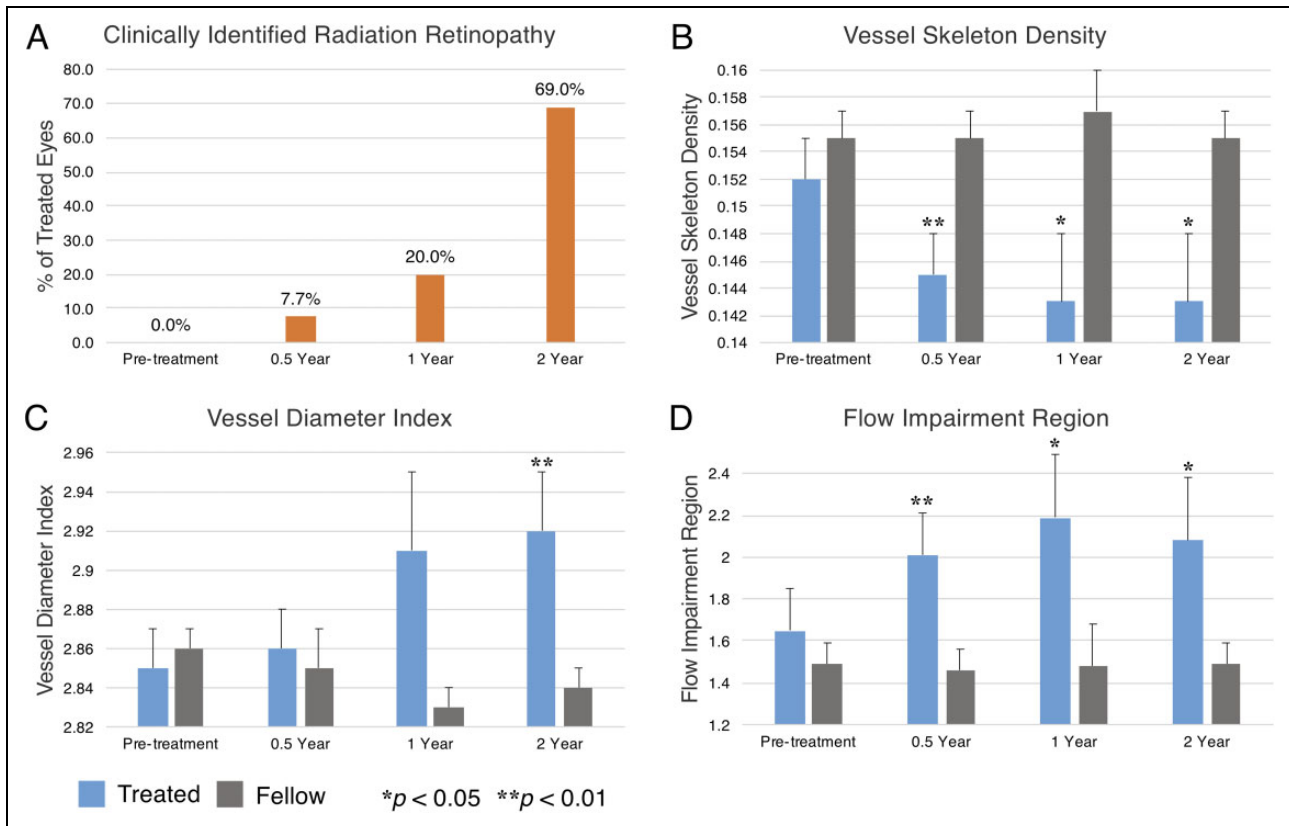


Figure 1. Longitudinal clinical and quantitative optical coherence tomography angiogram (data). All panels reflect data from our overall cohort. (A) Over the course of our 2-year follow-up period, there was an increasing percentage of treated eyes with clinically identifiable RR at each interval. Compared with fellow eyes over this period, treated eyes showed (B) decreasing vessel skeleton density, (C) increasing vessel diameter index, and (D) increasing flow impairment region. Relative significance between treated and fellow eyes at each time point is marked by asterisks, and error bars reflect SEM.

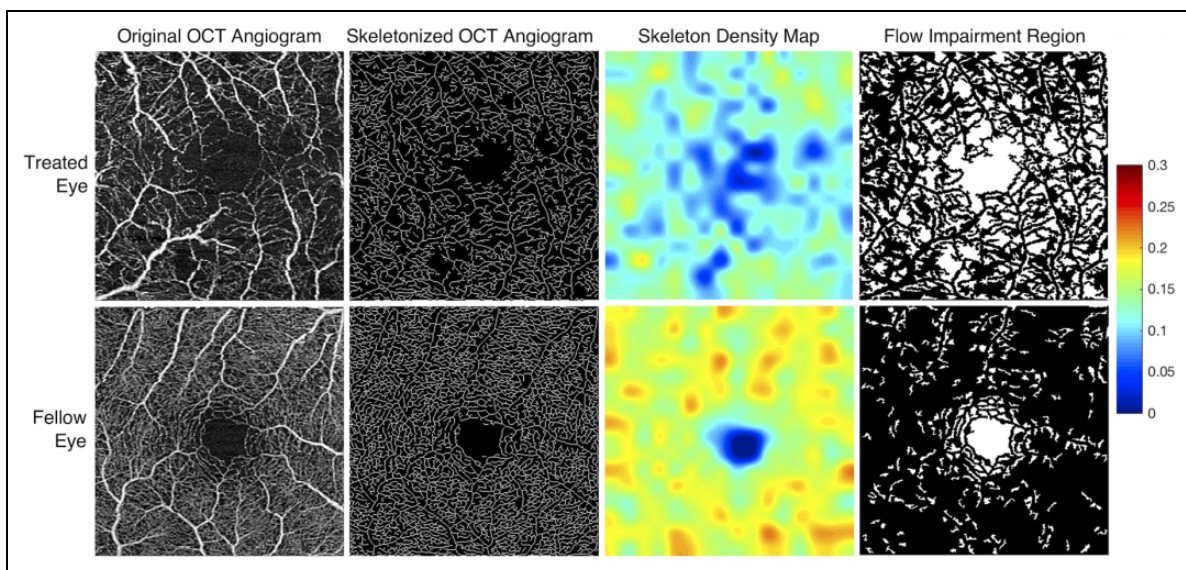


Figure 2. Processed optical coherence tomography angiograms (OCTAs) from treated and fellow eyes of a single patient. OCTAs from the treated (left eye) and fellow eye (right eye) of a 20-year-old woman demonstrate marked qualitative differences in parafoveal vessel density (column 1). The OCTA of each eye was obtained 263 days (8.6 months) following placement in the treated eye of a 46.0-Gy dose at the fovea. Visual acuity at the time of image acquisition was 20/350 in the treated eye and 20/20 in the fellow eye. Skeletonized OCTAs with accompanying skeleton density heat maps were generated (columns 2 and 3). Warmer colors reflect areas of greater vessel skeleton density, with relative differences defined on the accompanying color scale demonstrating decreased vessel skeleton density in the treated eyes. Pseudocolor flow impairment maps (column 4) demonstrate absent flow signal (white areas). The flow impairment region was markedly increased in the treated eye.

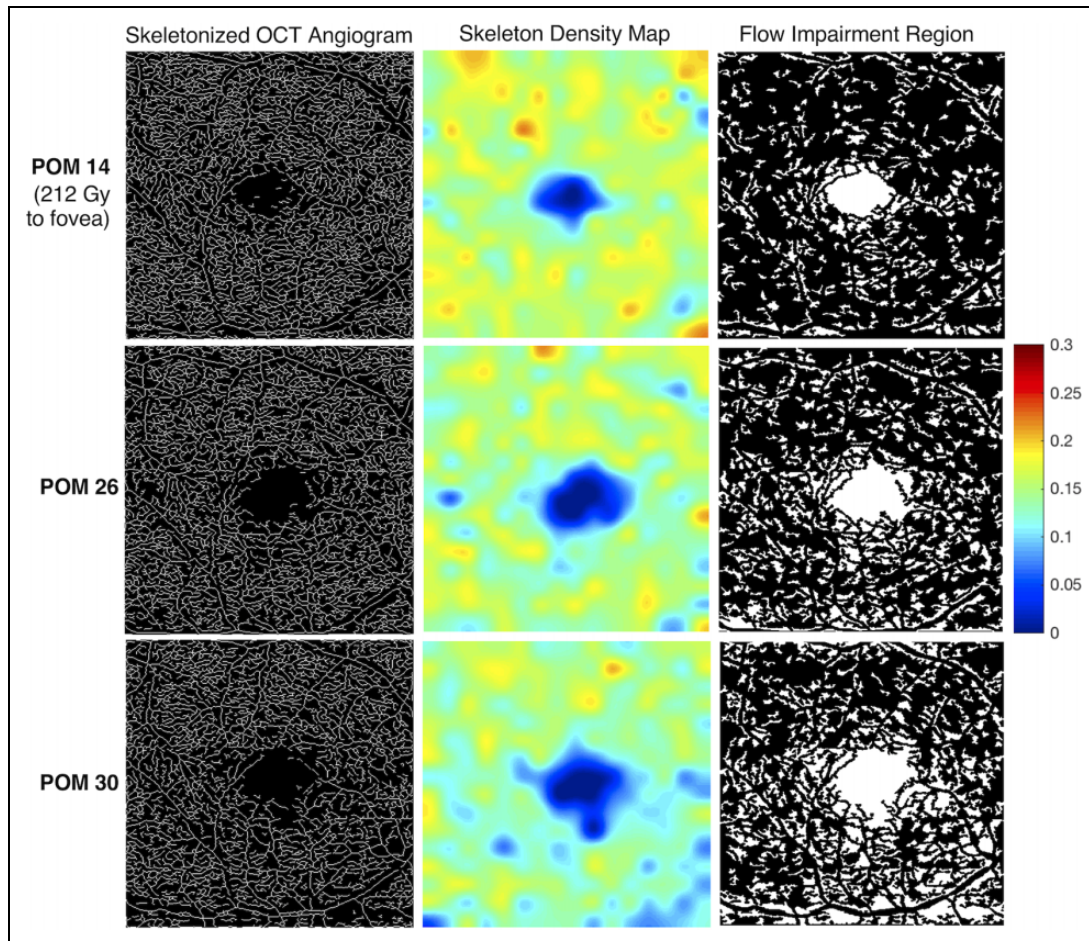


Figure 3. Longitudinal skeleton density and flow impairment maps of a treated eye. (Case 1) A 65-year-old man received 212 Gy to the fovea (right eye), with a range of 85 Gy to 250 Gy across the standard 3×3 -mm optical coherence tomography angiogram (OCTA). OCTAs were acquired at postoperative months (POMs) 14, 26, and 30. The visual acuity of the treated eye at these dates was 20/25, 20/25, and 20/80, respectively. The visual acuity of the fellow eye at the same time points (OCTA images not shown) was 20/25, 20/20, and 20/25, respectively. In the skeletonized image, impaired perfusion is visible inferiorly at POM 26 compared with POM 14, with worsening perfusion at POM 30 (column 1). The loss of skeleton density is more clearly visualized in the heat map at POM 26 (column 2). Warmer colors reflect areas of greater vessel skeleton density, with relative differences defined on the color scale. A parallel trend is seen in the flow impairment region images (column 3).

California.²³⁻²⁵ For each case, dosimetry maps were superimposed on both the original OCTAs and their corresponding fundus photographs for analysis.

Results

We report the results of 61 participants who underwent EPB therapy. Table 1 summarizes the demographic and clinical characteristics of the study population, as well as tumor and treatment characteristics. Table 2 summarizes the results of the OCTA metrics compared between EPB-treated and untreated fellow eyes.

Baseline

In total, 33 OCTAs of eyes with melanoma and fellow eyes were analyzed prior to EPB. Eyes with melanoma had

significantly lower VA compared with fellow eyes; however, there were no significant differences in VSD, VDI, or FIR (see Table 2).

Six-Month Follow-up

Thirty-two OCTAs of treated and fellow eyes were analyzed at 6 months after EPB (see Table 2). Among the treated eyes, only 1 (7.7%) demonstrated evidence of RR on clinical examination (Figure 1A). However, the VSD and FIR metrics of OCTA assessment showed significantly lower VSD and higher FIR for the treated eyes compared with fellow eyes (Table 2). These changes can also be appreciated qualitatively in maps of VSD and FIR (Figure 2). Importantly, among treated eyes with no clinically identifiable RR at this follow-up period that had pretreatment examinations for direct comparison ($n = 5$), there

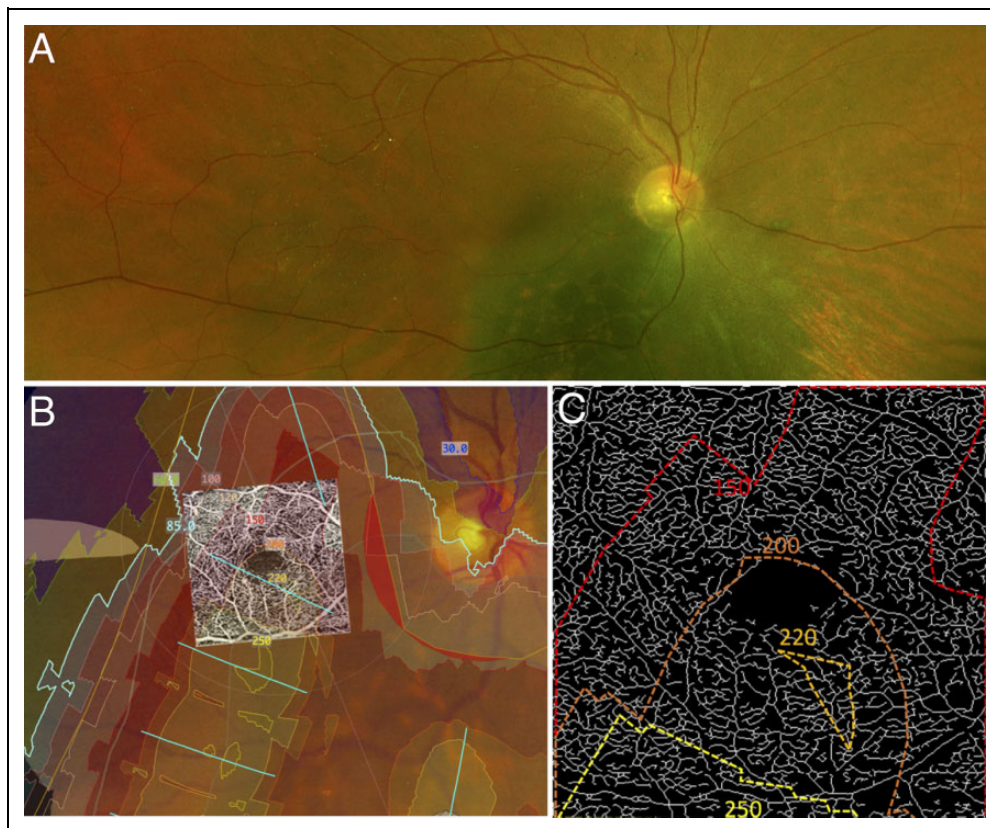


Figure 4. Spatial correlation of parafoveal microvascular changes with radiation dose. (A) The pretreatment fundus image of an individual (case 1) showing the choroidal melanoma. (B) A computed dosimetry simulation projected onto the pretreatment fundus image. A 3×3 -mm optical coherence tomography angiogram of the eye was registered with the image using vessel bifurcation landmarks. Dosimetry contour lines and dosimetry tints delineate areas of the eye that received specific doses of radiation from the plaque. (C) An enlarged skeletonized 3×3 -mm optical coherence tomography angiogram of the eye at postoperative month 30 with the corresponding dosimetry contour lines. Note the inferior areas of decreased vascular density (impaired perfusion) in the 3×3 -mm image, which corresponds with the higher doses delivered inferiorly.

was still a significantly decreased VSD (0.146 ± 0.011 [6 months] vs 0.158 ± 0.005 [baseline]; $P = .04$) and an increased FIR (1.76 ± 0.665 [6 months] vs 1.28 ± 0.339 [baseline]; $P = .04$).

One-Year Follow-up

In total, 30 OCTAs of treated and fellow eyes were analyzed at 12 months after EPB (see Table 2). Among the treated eyes, 3 (20%) demonstrated evidence of RR on clinical examination (see Figure 1A). Treated eyes also showed a significantly lower VSD and higher FIR compared with fellow eyes (see Table 2).

Two-Year Follow-up

In total, 32 OCTAs of treated and fellow eyes were analyzed at 24 months after EPB (see Table 2). Among the treated eyes, 9 (69%) demonstrated evidence of RR on clinical examination (see Figure 1A). Treated eyes showed a significantly lower VSD, higher VDI, and higher FIR compared with fellow eyes (Table 2). In general, the difference in all metrics between

treated and fellow eyes grew over time and corresponded with increasing rates of clinically identifiable RR in treated eyes (see Figure 1).

Impact of Vascular Comorbidities on Analyses

In our cohort 6 (9.8%) patients had diabetes without retinopathy. When these patients were excluded from our analysis, there was no loss of significance in VSD, VDI, and FIR at the intervals noted in Table 2. Also, in our overall cohort, 19 (31.1%) patients had a history of hypertension. In a GEE regression model that included age, VSD, and hypertension as independent variables and development of clinically evident RR as the dependent variable, VSD was significant ($P = .02$) whereas hypertension ($P = .60$) and age ($P = .40$) were not.

Radiation Dose Correlation With OCTA Changes

We found significant differences in the OCTA metrics VSD and FIR over the follow-up period when the overall cohort was divided into high-dose and low-dose foveal radiation

subgroups (>45 Gy [$n=9$] vs <15 Gy [$n=3$]): VSD (0.145 ± 0.002 [high dose] vs 0.154 ± 0.001 , $P<.001$) and FIR (2.04 ± 0.10 [high dose] vs 1.59 ± 0.06 , $P<.001$). The VDI metric was however not significantly different between the high-dose and low-dose classification (2.88 ± 0.02 [high dose] vs 2.83 ± 0.08 , $P=.21$).

Five 3×3 -mm OCTAs were selected for our exploratory within-eye dose-response analysis and had the following ranges of radiation dose across the fovea: case 1, 85 Gy to 250 Gy; case 2, 30 Gy to 70 Gy; case 3, 25 Gy to 60 Gy; case 4, 40 Gy to 60 Gy; and case 5, 8 Gy to 12 Gy. Of these, the case with the greatest radiation gradient across the fovea (case 1) had an EPB dosimetry gradient that qualitatively correlated with the spatial microvascular gradient on the 3×3 -mm OCTA. The longitudinal OCTA findings of case 1 are illustrated in Figure 3, and the registered EPB dosimetry map and OCTA microvasculature are illustrated in Figure 4. The dose-dependent nature of impaired perfusion over time can be appreciated from Figure 3 when the EPB dosimetry map in Figure 4 is taken into account. The remaining cases did not appear to have any spatially correlated microvascular changes within the 3×3 -mm window.

Conclusions

This study adds to a body of literature that has demonstrated retinal microvascular changes after EPB. Specifically, our study demonstrated a significant decrease in capillary density in EPB-treated eyes earlier than previously reported and prior to clinically evident RR. It also showed progressive decreases in capillary density at intervals over a 2-year period. This was accomplished using quantitative metrics that reflect microvascular density directly, such as VSD, and indirectly, such as FIR. Significant increases in VDI were also seen over this period, which likely correspond to dropout of small-caliber capillaries. In addition to these findings, we demonstrate that radiation dose to the fovea is a significant predictor of VSD and FIR. In one idealized case we were able to show a large gradient (>165 Gy) of high-dose radiation across the fovea that appears to be spatially correlated to microvascular density. Collectively, these data suggest that capillary changes are occurring before clinically evident retinopathy, and that the magnitude of the radiation dose may correlate with the magnitude of the capillary damage in any given region. Furthermore, they highlight the potential utility of OCTA to monitor the progression of subtle changes in microvasculature over a period of months in treated eyes.

Our findings are consistent with those in prior studies that used OCTA to assess parafoveal vessel density in irradiated eyes. Say et al and Cennamo and colleagues quantified total vascular area using 3×3 - and 6×6 -mm binarized en face images, respectively.^{14,15} Both demonstrated significant reduction in vessel area density in irradiated eyes compared with fellow eyes. Although the capillary densities in these previous studies were estimated as vessel area density, our preferred method for estimating capillary density is the skeletonized

density (VSD). This is because VSD is not influenced by capillary morphologic changes such as vessel diameter, which may accompany vasculopathies, and is also minimally affected by large-caliber vessels.

For brevity, our study reports only the VSD analysis as the measure of capillary density. Vessel diameter was approximated as an index, VDI, which we also demonstrated changes with worsening retinopathy. FIR, our third metric, complements VSD as an indirect measure of density and a direct measure of sub-clinical impaired perfusion. As FIR accounts only for avascular areas larger than a set threshold, it theoretically has a higher specificity (but lower sensitivity) for capillary dropout. For example, the loss of minute areas of capillary flow may not result in an avascular area greater than our set threshold and therefore would have no effect on FIR but a definite effect on VSD.

The findings of our study highlight the potential use of OCTA for monitoring vascular changes in irradiated eyes over time. The vascular metrics can also serve as adjuncts to help grade the severity of RR. Several groups have aimed to develop effective grading schemes for RR that use various imaging modalities, including ultra-widefield fluorescein angiography.⁹ In 2005, Finger and Kurli developed a system with 4 stages of severity that correlated with vision loss, based on a combination of findings from dye-based angiography and ophthalmoscopy.⁸ Horgan et al later described in 2008 how OCT could be further added to identify ME, an early clinical feature of RR.⁷ More recently, Veverka and colleagues suggested OCTA could also be used to help grade severity, demonstrating that it may detect RR prior to changes seen on OCT alone.²⁶

Thus, we concur with the assertion that OCTA may be a powerful tool in determining the severity of RR and detecting very early microvascular changes before the onset of retinopathy on examination. This has a wide variety of clinical applications. The use of various metrics as demonstrated in this study may noticeably increase the sensitivity of OCTA to capture early changes in RR, because subtle changes in density and vessel diameter are often challenging to appreciate qualitatively in the clinic setting. For clinical purposes, we suggest obtaining 3×3 -mm OCTAs in both eyes prior to EPB placement and intermittently at follow-up visits for those with access to these devices. As our study has shown, significant microvascular changes can be seen within 6 months of treatment, suggesting repeated imaging may be prudent even at early postoperative dates.

Furthermore, as our understanding of the utility of OCTA continues to grow, longitudinal scans may prove useful in individualizing the time point for initiating RR treatment, such as when VSD or FIR reaches a certain threshold value. Given recent studies evaluating earlier (or even prophylactic) antivascular endothelial growth factor therapy for RR, these reproducible, quantitative OCTA measures may thus provide sensitive biomarkers for comparing the efficacy of RR treatment regimens.²⁷⁻³⁰

Our exploration of a possible spatial correlation between radiation dose and capillary density was demonstrated in case

1 (see Figure 4), which had, by chance alone, a steep gradient change for the radiation dose over the 3×3 -mm area of the macula that was imaged. As already noted, the tumor in this case appears to partially overlap with the inferonasal edge of the 3×3 -mm window, which may confound the analysis. However, there were not any segmentation errors or other subjective abnormalities on the OCTA of this individual that would explain the gradient of changes observed. Of note, case 4 also showed a large area of ischemia nearest the high-dose radiation in a wider 6×6 -mm window. The significantly lower resolution of 6×6 -mm OCTA scans precludes a detailed analysis of density changes in these scans. Our findings provide a basis for future studies to assess the within-eye spatial relationship between EPB dosimetry and microvasculature abnormalities and enhance the understanding of radiation dose on the retinal vasculature and the development of RR.

Because DR shares many clinical features of RR, we further performed an analysis on our cohort after excluding our 6 patients with diabetes, none of whom had preexisting DR. With exclusion of these patients, there was no loss of significance in any metrics for each time interval detailed in Table 2. As such, the inclusion of patients with diabetes does not change our conclusions. However, a larger study with more people with diabetes may reveal that the disease affects the rate of progression of vascular change or the likelihood of treated eyes developing RR over the long term.

Furthermore, hypertension may similarly affect the progression of vascular change. With a large number of patients with hypertension in our cohort, we performed a GEE regression analysis that included hypertension, age, and VSD, with development of RR as the end point. Whereas VSD was found to be significant, hypertension was not. However, as with diabetes, a larger study is likely needed to identify any role of hypertension with greater certainty.

Some potential limitations of our study include those inherent to OCTA imaging, such as motion artifacts and floaters, which can interfere with efforts to accurately quantify vascular metrics. We aimed to control this by excluding images with significant artifacts. Furthermore, because single OCTA scans may miss capillaries that are only intermittently perfused, FIR may overestimate the number of truly nonperfused areas greater than our set threshold, which in future analysis could be addressed by image averaging. Additionally, this study analyzed images from the 3×3 -mm OCTA scan pattern and may have missed some peripheral defects associated with EPB. However, larger scan patterns available at the time of this study did not have sufficient resolution to reliably detect capillary level changes, so use of the high-resolution 3×3 -mm field was necessary. Future studies may consider images from 6×6 -mm or even larger windows if the resolution of the scans is sufficient. Furthermore, future studies may aim to generate dosimetry maps in a larger number of eyes and use more quantitative approaches to better evaluate the spatial relationship between EPB dosimetry and microvascular aberrations.

Other limitations arise from the retrospective nature of the data analyzed. For example, the images for the study

were acquired during study visits that were determined on a case-by-case basis by the physician. Although we addressed the difference in the time intervals by binning, our findings can be refined by using regularized and standardized follow-up intervals across participants. Finally, we acknowledge that radiation may not be the only etiology of vasculopathy that is observed in RR, especially in affected areas that received sub-threshold radiation. For example, a tumor itself may induce ischemia in a larger vessel that would affect distal vasculature. Likewise, it could do the same to a major vascular arcade that would affect distal macular vasculature, although we saw no evidence of this in any case.

In conclusion, we investigated OCTA changes associated with EPB treatment of choroidal melanoma and found significant changes in OCTA metrics at about 6 months or earlier, even when there were no clinically detectable signs of RR. The change in the OCTA metrics increased over time and in a dose-dependent manner. We infer that OCTA can be a viable tool for monitoring the effect of EPB on the retinal microvasculature, and its findings may play a pivotal role in developing intervention modalities to delay or treat the occurrences of retinopathy after EPB.

Authors' Note

This work was presented at the American Society of Retina Specialists Annual Meeting, Vancouver, British Columbia, July 22, 2018.

Ethical Approval

This article was conducted in accordance with the Declaration of Helsinki. Approval for this study was obtained from the institutional review board of the University of Southern California. The collection and evaluation of all protected patient information was performed in a HIPPA (Health Insurance Portability and Accountability Act)-compliant manner.

Statement of Informed Consent

Informed consent was obtained prior to performing the procedure, including permission for publication of all photographs and images included herein.

Declaration of Conflicting Interests

The author(s) declared the following potential conflicts of interest with respect to the research, authorship, and/or publication of this article: A.H.K. and R.K.W. have received grant support and honoraria from Carl Zeiss Meditec. M.A.A. has controlling interest in Eye Physics LLC. The other authors have nothing to declare.

Funding

The author(s) disclosed receipt of the following financial support for the research, authorship, and/or publication of this article: This work was supported by the National Institutes of Health (grant numbers R01EY030564, 1K08EY027006, R01EY028753, and K08CA232344); Carl Zeiss Meditec; and unrestricted University of Southern California Roski Eye Institute departmental funding from Research to Prevent Blindness.

ORCID iD

Amir H. Kashani, MD, PhD  <https://orcid.org/0000-0001-9767-7920>

References

1. Collaborative Ocular Melanoma Study Group. The COMS randomized trial of iodine 125 brachytherapy for choroidal melanoma: V. Twelve-year mortality rates and prognostic factors: COMS report No. 28. *Arch Ophthalmol.* 2006;124(12):1684-1693. doi:10.1001/archophth.124.12.1684
2. Melia BM, Abramson DH, Albert DM, et al; Collaborative Ocular Melanoma Study Group. Collaborative ocular melanoma study (COMS) randomized trial of I-125 brachytherapy for medium choroidal melanoma. I. Visual acuity after 3 years COMS report No. 16. *Ophthalmology.* 2001;108(2):348-366. doi:10.1016/s0161-6420(00)00526-1
3. Berry JL, Dandapani SV, Stevanovic M, et al. Outcomes of choroidal melanomas treated with Eye Physics: a 20-year review. *JAMA Ophthalmol.* 2013;131(11):1435-1442. doi:10.1001/jamaophthalmol.2013.4422
4. Le BHA, Kim JW, Deng H, et al. Outcomes of choroidal melanomas treated with Eye Physics plaques: a 25-year review. *Brachytherapy.* 2018;17(6):981-989. doi:10.1016/j.brachy.2018.07.002
5. Durkin SR, Roos D, Higgs B, Casson RJ, Selva D. Ophthalmic and adnexal complications of radiotherapy. *Acta Ophthalmol Scand.* 2007;85(3):240-250. doi:10.1111/j.1600-0420.2006.00822.x
6. Archer DB, Amoaku WM, Gardiner TA. Radiation retinopathy—clinical, histopathological, ultrastructural and experimental correlations. *Eye (Lond).* 1991;5(pt 2):239-251. doi:10.1038/eye.1991.39
7. Horgan N, Shields CL, Mashayekhi A, Teixeira LF, Materin MA, Shields JA. Early macular morphological changes following plaque radiotherapy for uveal melanoma. *Retina.* 2008;28(2):263-273. doi:10.1097/IAE.0b013e31814b1b75
8. Finger PT, Kurli M. Laser photocoagulation for radiation retinopathy after ophthalmic plaque radiation therapy. *Br J Ophthalmol.* 2005;89(6):730-738. doi:10.1136/bjo.2004.052159
9. McCannel TA, Kim E, Kamrava M, et al. New ultra-wide-field angiographic grading scheme for radiation retinopathy after iodine-125 brachytherapy for uveal melanoma. *Retina.* 2018;38(12):2415-2421. doi:10.1097/IAE.0000000000001874
10. Kashani AH, Chen CL, Gahm JK, et al. Optical coherence tomography angiography: a comprehensive review of current methods and clinical applications. *Prog Retin Eye Res.* 2017;60:66-100. doi:10.1016/j.preteyeres.2017.07.002
11. Kim AY, Chu Z, Shahidzadeh A, Wang RK, Puliafito CA, Kashani AH. Quantifying microvascular density and morphology in diabetic retinopathy using spectral-domain optical coherence tomography angiography. *Invest Ophthalmol Vis Sci.* 2016;57(9):OCT362-OCT370. doi:10.1167/iovs.15-18904
12. Koullis N, Kim AY, Chu Z, et al. Quantitative microvascular analysis of retinal venous occlusions by spectral domain optical coherence tomography angiography. *PLoS One.* 2017;12(4):e0176404. doi:10.1371/journal.pone.0176404
13. Kim AY, Rodger DC, Shahidzadeh A, et al. Quantifying retinal microvascular changes in uveitis using spectral-domain optical coherence tomography angiography. *Am J Ophthalmol.* 2016;171:101-112. doi:10.1016/j.ajo.2016.08.035
14. Say EA, Samara WA, Khoo CT, et al. Parafoveal capillary density after plaque radiotherapy for choroidal melanoma: analysis of eyes without radiation maculopathy. *Retina.* 2016;36(9):1670-1678. doi:10.1097/IAE.0000000000001085
15. Cennamo G, Breve MA, Velotti N, et al. Evaluation of vascular changes with optical coherence tomography angiography after plaque radiotherapy of choroidal melanoma. *Ophthalmic Res.* 2018;60(4):238-242. doi:10.1159/000490571
16. Parrozzani R, Frizziero L, Londei D, et al. Peripapillary vascular changes in radiation optic neuropathy: an optical coherence tomography angiography grading. *Br J Ophthalmol.* 2018;102(9):1238-1243. doi:10.1136/bjophthalmol-2017-311389
17. Skalet AH, Liu L, Binder C, et al. Quantitative OCT angiography evaluation of peripapillary retinal circulation after plaque brachytherapy. *Ophthalmol Retina.* 2018;2(3):244-250. doi:10.1016/j.oret.2017.06.005
18. Chu Z, Lin J, Gao C, et al. Quantitative assessment of the retinal microvasculature using optical coherence tomography angiography. *J Biomed Opt.* 2016;21(6):66008. doi:10.1117/1.JBO.21.6.066008
19. Berry JL, Kim JW, Jennelle R, Astrahan M. Use of the toric surgical marker to aid in intraoperative plaque placement for the USC Eye Physics plaques to treat uveal melanoma: a new surgical technique. *Ophthalmic Surg Lasers Imaging Retina.* 2015;46(8):866-870. doi:10.3928/23258160-20150909-12
20. Michaelson IC. *Retinal Circulation in Man and Animals.* Thomas Publisher; 1954.
21. Ying GS, Maguire MG, Glynn R, Rosner B. Tutorial on biostatistics: statistical analysis for correlated binary eye data. *Ophthalmic Epidemiol.* 2018;25(1):1-12. doi:10.1080/09286586.2017.1320413
22. Grimm J, LaCouture T, Croce R, Yeo I, Zhu Y, Xue J. Dose tolerance limits and dose volume histogram evaluation for stereotactic body radiotherapy. *J Appl Clin Med Phys.* 2011;12(2):3368. doi:10.1120/jacmp.v12i2.3368
23. Astrahan MA, Luxton G, Jozsef G, et al. An interactive treatment planning system for ophthalmic plaque radiotherapy. *Int J Radiat Oncol Biol Phys.* 1990;18(3):679-687. doi:10.1016/0360-3016(90)90077-w
24. Astrahan MA, Luxton G, Pu Q, Petrovich Z. Conformal episcleral plaque therapy. *Int J Radiat Oncol Biol Phys.* 1997;39(2):505-519. doi:10.1016/s0360-3016(97)00118-1
25. Astrahan MA. Improved treatment planning for COMS eye plaques. *Int J Radiat Oncol Biol Phys.* 2005;61(4):1227-1242. doi:10.1016/j.ijrobp.2004.09.062
26. Veverka KK, AbouChehade JE, Iezzi R, Pulido JS. Noninvasive grading of radiation retinopathy: the use of optical coherence tomography angiography. *Retina.* 2015;35(11):2400-2410. doi:10.1097/IAE.0000000000000844

27. Murray TG, Latiff A, Villegas VM, Gold AS. Aflibercept for radiation maculopathy study: a prospective, randomized clinical study. *Ophthalmol Retina*. 2019;3(7):561-566. doi:10.1016/j.oret.2019.02.009
28. Stacey AW, Demirci H. Serial intravitreal bevacizumab injections slow the progression of radiation maculopathy following iodine-125 plaque radiotherapy. *Open Ophthalmol J*. 2016;10:103-110. doi:10.2174/1874364101610010103
29. Houston SK, Shah NV, Decatur C, et al. Intravitreal bevacizumab combined with plaque brachytherapy reduces melanoma tumor volume and enhances resolution of exudative detachment. *Clin Ophthalmol*. 2013;7:193-198. doi:10.2147/OPHTH.S37938
30. Shah SU, Shields CL, Bianciotto CG, et al. Intravitreal bevacizumab at 4-month intervals for prevention of macular edema after plaque radiotherapy of uveal melanoma. *Ophthalmology*. 2014;121(1):269-275. doi:10.1016/j.ophtha.2013.08.039